

A Model for the Prediction of the Performance of a Spined-Tube Absorber—Part 2: Model and Results

A. Terrence Conlisk, Ph.D.

ABSTRACT

In this paper a model for the heat and mass transport on a vertically oriented spiny tube is developed based on the dimensional analysis given in part 1. It is shown that when the influence of surface tension is neglected between the spines, there is an enhancement of the mass transfer rate to the liquid film; however, the enhancement is not large. It is suggested that the enhancement is due to the generation of a variation of the mass fraction on the local spine scale. The influence of the coolant flow is incorporated as well, and the model may thus be used in conjunction with a cycle analysis to determine whether given absorber states may be attained. Experimental results show that when the pitch of the spines is decreased, the performance of the tube is significantly degraded and the spines actually inhibit mass transfer. A physical reason for this, based on the influence of surface tension through capillary effects, is advanced.

INTRODUCTION

This paper examines the nature of the flow and heat and mass transfer on a spiny tube of a given dimension. A model to predict the total mass absorbed on the tube and other relevant design quantities is developed based on the dimensional analysis of the problem described in part 1 (Conlisk 1996); the nature of the flow and heat and mass transfer on the tube depends on the relative magnitude of a number of dimensionless parameters. As noted in part 1 (Conlisk 1996), there are three major objectives of this work:

1. to develop a relatively simple model,
2. to minimize or eliminate the use of free constants, and
3. to minimize the amount of computing power required.

The model may be executed on a personal computer, with the solution for a single design point taking only seconds to run. The present model takes full advantage of the existence of closed-form, analytical solutions for the mass fraction, temperature, and flow velocity.

The model for the absorption problem on the spiny tube is based upon analysis of two regions of interest. In the region between the spine rows, it is assumed that the influence of the spines themselves is negligible and the heat and mass transfer problems are governed by the global variables of total flow rate and total length of tube. In the region between a pair of spines on a given spine row, heat and mass transfer problems are governed by the pitch of the spine tube, defined as the distance between spine rows (Conlisk 1996). Between a pair of spines, it is assumed that the wall temperature is constant because the root chord of the spines is so short and a closed form for the mass absorbed there may be obtained. The root chord of a spine is the length of the spine in the primary flow direction at the base of the spine (Conlisk 1996).

In past work by the author (Conlisk 1992, 1994a, 1994b, 1994c, 1994d, 1995), the wall temperature is required to be specified. To eliminate this requirement, the coolant-side problem has been formulated and coupled with the film side. In this way, the entire absorber system is modeled; a countercurrent mode of operation is assumed. The model is subject only to the specification of a single coolant-side heat transfer coefficient and, in the absence of surface tension effects, no other free constants need to be specified. The model requires only the numerical calculation of two integrals and thus a minimum of numerical work is required.

The plan of this paper is as follows. Using the results of part 1, the coolant flow problem is formulated in the next section. Next, the spiny tube model is developed and results for the outlet mass fraction and temperature and absorbed mass flux are presented. The influence of surface tension is discussed in the following section.

A. Terrence Conlisk is an associate professor in the Department of Mechanical Engineering at Ohio State University, Columbus.

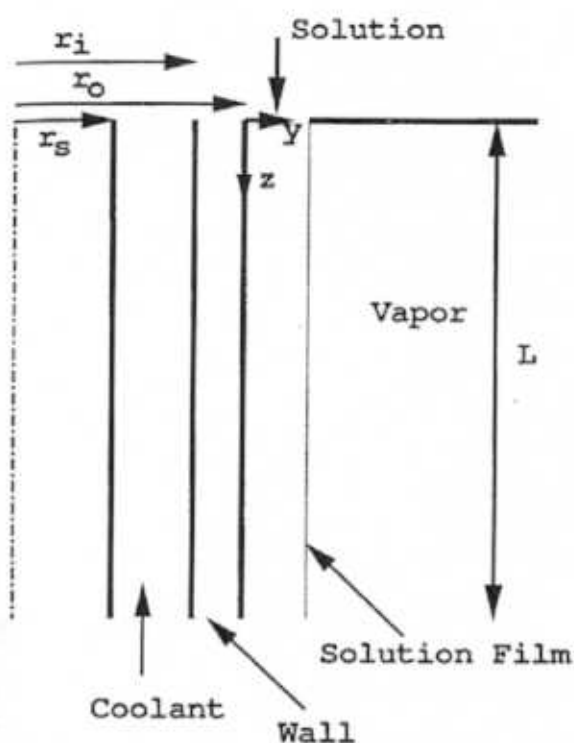


Figure 1 Geometry showing the coolant side and film side in cross section. The solution film thickness is greatly expanded. The spines are not shown in this figure.

COOLANT FLOW

The nature of the coolant flow problem is considered and how it is coupled with the solution side. All the variables are nondimensionalized based on global variables: the total length of the tube (L) and the velocity (U_0) based on total flow rate. The analysis here is similar to that discussed by Conlisk (1995) and the same notation is used for many of the variables. Using the standard heat balance in the tube (Incropera and DeWitt 1990), the coolant-side bulk temperature is defined by the equation

$$\dot{m}_{cool} c_{pcool} \frac{dT_{BC}}{dz} = q_s A_r \quad (1)$$

where

A_r = heat transfer area on the solution side,

q_s = heat flux,

T_{BC} = bulk temperature on the coolant side,

\dot{m}_{cool} = coolant mass flow rate, and

c_{pcool} = coolant specific heat.

z measures the dimensionless distance from the top of the tube (Figure 1). In the experiments, the coolant flow passage is an annulus with an inside radius, r_s , and an outside radius, r_i (the

inside wall radius); this is depicted in Figure 1. Since convection of heat is neglected on the solution side and conduction also dominates through the tube wall, the dimensional heat flux is

$$q_s = \dot{m}_{abs}^* h_{abs} = \alpha \delta^{1/2} \epsilon_B \rho U_0 \dot{m}_a \theta h_{abs} \quad (2)$$

Note that the energy flux at the interface is assumed to be composed of the latent heat released in the phase-change process because convection in the vapor is small, as noted in part 1. Solving for the bulk temperature in the coolant using Equation 1,

$$T_{BC}(z) - T_{BCin} = E' \{h_1(1) - h_1(z)\}, \quad (3)$$

where

$$E' = \frac{\alpha \delta^{1/2} B \epsilon \rho U_0 h_{abs} A_r}{\dot{m}_{cool} c_{pcool}} \quad (4)$$

Equation 3 expresses the important result that the rise in bulk temperature is directly proportional to the increase in perturbation film thickness. Note that this equation contains no adjustable parameters; however, to actually calculate the perturbation film thickness, the film-side heat transfer coefficient must be specified. This is discussed next.

The temperature distribution within the tube wall is conduction-dominated and in dimensional form, with r measured from the centerline of the tube (Figure 1):

$$T = (T_W - T_{WC}) \frac{\ln\left(\frac{r}{r_o}\right)}{\ln\left(\frac{r_o}{r_i}\right)} + T_W \quad (5)$$

where T_W is the wall temperature on the film side and T_{WC} is the wall temperature on the coolant side. By balancing the heat load at the wall on the solution side, one obtains

$$T_W - T_{WC} = \frac{\alpha r_o \ln(r_o/r_i) \rho U_0 \delta^{1/2} B \epsilon \dot{m}_a \theta h_{abs}}{k_w} \quad (6)$$

where k_w is the conductivity of the wall.

Nondimensionalizing Equation 3, one gets

$$\begin{aligned} \theta_{BC} &= \frac{T_{BC} - T_{WIn}}{\Delta T} \\ &= \theta_{Bin} + \frac{E'}{\Delta T} (h_1(1) - h_1(z)). \end{aligned} \quad (7)$$

ΔT is the difference between the film surface and wall temperatures at the inlet on the solution side. Balancing the heat load at the wall on the coolant side,

$$T_W(z) = T_{BC}(z) - \dot{m}_a \theta \quad (8)$$

where γ is defined by

$$\gamma = \frac{\alpha \rho U_0 \delta^{1/2} B \epsilon h_{abs} \left[\frac{r_o}{r_i} + \frac{h_c t}{k_w} \right]}{h_c} \quad (9)$$

Now from the conduction-dominated temperature distribution and the boundary condition at the interface discussed in part 1, on the film side

$$\theta_s = \theta_w - A \dot{m}_{a0} \quad (10)$$

where $A = (\delta^{1/2} B \alpha \epsilon Re Pr) / Ja$. Using Equation 7 in dimensionless form and the equilibrium condition at the interface,

$$\theta_s = \theta_{BC} - A' \dot{m}_{a0} \quad (11)$$

and

$$\Omega_s = \frac{1}{C} \theta_{BC} - \frac{A'}{C} \dot{m}_{a0} + \beta \quad (12)$$

with $A' = A + \gamma$ and $C = \Delta \omega / C_1 \Delta T$. Substituting the solution for the mass fraction (Equation 26 in part 1) into Equation 12 and using Equation 7, an integral equation for the mass absorbed emerges and the equation is given by

$$\int_0^z \frac{\dot{m}_{a0} dt}{(z-t)^{1/2}} = -\frac{1}{\sqrt{2} C \alpha} \left(\frac{E'}{\Delta T} \int_0^z \dot{m}_{a0} dt - A' \dot{m}_{a0} \right) + \beta \quad (13)$$

Taking the Laplace transform of Equation 13, solving for \dot{m}_{a0} in the transform plane, and then inverting yields

$$\dot{m}_{a0} = -\frac{H}{\pi |D_1|} \left[\int_0^{\infty} \frac{\sqrt{x} e^{-xz} dx}{\left(x + \frac{E'}{A' \Delta T}\right)^2 + \frac{x}{D_1^2}} + \frac{\pi |D_1| e^{s_0 z}}{1 + \frac{1}{2\sqrt{s_0} |D_1|}} \right] \quad (14)$$

where H is a parameter defined by

$$H = \frac{C}{A'} \beta + \frac{T_{BCout} - T_{Win}}{A' \Delta T} \quad (15)$$

s_0 is the position of the pole of the function

$$f(s) = s - \frac{E'}{A' \Delta T} + s^{1/2} / |D_1|,$$

where s is the complex variable for the Laplace inversion. To obtain the bulk coolant temperature, the film thickness is required and from the above expression for the mass flux, the result is

$$h_1(z) = \frac{H}{\pi |D_1|} \int_0^{\infty} \frac{(e^{-xz} - 1) dx}{\sqrt{x} \left(x + \frac{E'}{A' \Delta T}\right)^2 + \frac{x}{D_1^2}} + \frac{H}{s_0 |D_1|} \frac{e^{s_0 z} - 1}{1 + \frac{1}{2\sqrt{s_0} |D_1|}} \quad (16)$$

In Equations 14 and 16, D_1 is a parameter defined by

$$D_1 = \frac{A'}{\alpha C} \left\{ \frac{1}{2} \right\}^{1/2}$$

The coolant side is incorporated by specifying the coolant mass flow rate, the specific heat, and the average heat transfer coefficient. In addition, the wall thickness and wall conductivity must be specified. However, it is noted that $\Delta T = T_{Sin} - T_{Win}$ is unknown until the coolant-side temperature is known. The standard Dittus-Boelter correlation (Incropera and Dewitt 1990) is used to calculate the coolant heat transfer coefficient (Miller 1993).

The only numerical calculation required is the evaluation of the integrals in Equations 14 and 16, which cannot be easily evaluated analytically. Recall that the calculations are based on the assumption that the temperature becomes conduction-dominated immediately upon entrance to the tube. The results of Conlisk (1992, 1995) suggest that this assumption is approximately correct, since the adjustment region is short. The wall and film surface temperatures are unknown and one of these must be iterated. As in Conlisk (1995), we iterate on the dimensionless film surface temperature (θ_s); a relative test is used with a convergence criterion of 10^{-4} . In general, the scheme converges in less than 10 iterations.

To test the accuracy of the model, results for the smooth tube were calculated and compared with the experiment; these results are given by Conlisk (1995). The results for all four data sets are good on the film side, although the temperature values at the outlet on both the film and coolant sides are somewhat under-predicted.

The calculation of the absorbed mass flux has been carried out in two ways. First, the absorbed flux has been calculated using the standard one-dimensional approach described in previous work (Conlisk 1992; Miller 1992). However, the absorbed mass flux can also be calculated using the two-dimensional analysis; the mass flux is directly related to the film thickness and the result for the total mass absorbed is

$$\int_0^1 \dot{m}_{a0} dz = -h_1(1), \quad (17)$$

where $h_1(1)$ is the film thickness at the outlet given by Equation 16. In the results of Conlisk (1995), the one-dimensional approach tends to overpredict the two-dimensional results.

At this point, all the preliminary work required for the development of the spiny tube model is complete. In particular,

the mass absorbed is considered to be a perturbation (not necessarily small) to the smooth-tube results in which an expression for the mass absorbed between the spines is required. The model is described next.

THE SPINY TUBE MODEL

The data in Table 2 of part 1 suggest that surface tension effects are effectively negligible for the tubes with a 1/4-in. pitch, a bit more important for the 3/16-in. pitch, and possibly a first-order effect for data sets ht3-1 and ht3-2; consequently, we begin by using the smooth-tube analysis of the previous section to build the spiny tube model. In the model, the total absorbed mass flux is considered to be the sum of a smooth-tube component plus a spiny tube component:

$$\dot{m}_a^* = A_{ra} \dot{m}_{as}^* + (1 - A_{ra}) \dot{m}_{asp}^* \quad (18)$$

where A_{ra} is the ratio of the total area of the tube minus the portion between the spine channels to the total surface area of the tube. The units of \dot{m}_a^* are, say, kg/m²/s. Thus, using the scaling parameters motivated by previous work (Conlisk 1992, 1994a) and with $\dot{M}_{aT} = \dot{m}_a^* / \rho U_0$, the dimensionless mass flux is thus given by

$$\begin{aligned} \dot{M}_{aT} &= \varepsilon \dot{m}_{aT} \\ &= \delta^{1/2} \varepsilon B \left\{ A_{ra} \dot{m}_{as0} + (1 - A_{ra}) \frac{\delta_{sp}^{1/2} \varepsilon_{sp}}{\delta^{1/2} \varepsilon} \dot{m}_{asp0} \right\} \quad (19) \end{aligned}$$

In Equation 19, it is assumed that each spine channel around the circumference contributes the same amount to the absorption process. If a mass absorption enhancement parameter is defined by

$$M_e = \frac{\delta_{sp}^{1/2} \varepsilon_{sp}}{\delta^{1/2} \varepsilon}$$

then Equation 19 may be written concisely as

$$\dot{M}_{aT} = \delta^{1/2} \varepsilon B \{ A_{ra} \dot{m}_{as0} + (1 - A_{ra}) M_e \dot{m}_{asp0} \} \quad (20)$$

The absorbed mass flux in the region between each pair of spine rows is given by Equation 14 in the global dimensionless variable z ; the global variable z is made dimensionless on the length of the tube. The spiny tube component of the mass flux is modeled based on the realization that as the solution passes between the spines, the local length scale is the pitch of the tube rather than the total length of the tube. Moreover, each spine channel carries only a small portion of the total mass flow down the tube. In addition, physical arguments suggest that the wall temperature difference through the spine channel will be very small. It is through the axially varying wall temperature difference that the influence of the coolant flow on the film is felt. The mass transfer in this region is likely to be driven by the lack of equilibrium between the bulk

of the film and the wall as characterized by the fact that $\beta \neq 0$. Here β is defined (Conlisk 1996) as

$$\beta = \frac{C_1 T_{Win} + C_2 - \omega_{ABULK}}{\Delta \omega} \quad (21)$$

Thus for use in Equation 19 we define

$$\dot{m}_{asp0} = \frac{C \beta}{A_{sp}} G(z) \quad (22)$$

where

$$G(z) = e^{\frac{1}{D_{1sp}} z} \operatorname{erfc} \left(\frac{\sqrt{z}}{D_{1sp}} \right) \quad (23)$$

where D_{1sp} and A_{sp} are parameters based on local spine quantities and are defined by

$$D_{1sp} = \sqrt{2} \frac{A_{sp}}{\alpha C}$$

and

$$A_{sp} = \frac{\delta_{sp}^{1/2} B \varepsilon_{sp} \operatorname{RePr} \alpha}{\operatorname{Ja}}$$

Equation 22 may be derived in smooth-tube variables by assuming that the wall temperature is locally constant so that in dimensionless terms $\theta_w = 0$. The solution is given in Conlisk (1995).

To begin the solution process, the geometrical parameters for the spiny tube are input and the dimensionless parameters are calculated. The number of points in the grid $nt = N_{st} + 1$, where N_{st} is the number of spine rows on the tube; thus, each grid point corresponds to the outlet of row i or the inlet to row $i + 1$ in the global coordinate system. The number of rows per six inches was measured by the author during a visit to a national laboratory; based on this measurement, for the 1/4-in. pitch, there are 240 spine rows; for the 3/16-in. pitch, there are 320 spine rows; and for the 1/8-in. pitch, there are 480 spine rows. The number of spine rows is related to the pitch by the equation

$$P_B = \frac{L - N_{st} L_{sp}}{N_{st}} \quad (24)$$

where L_{sp} is the root chord of the spine in the primary flow direction and has been measured to be about 1/32 in. The pitch of the tubes is defined as $P = P_B + L_{sp}$. Use of Equation 24 for P_B allows variation of the chord of the spines while keeping the pitch the same.

The numerical procedure used for the spiny tube is the same as discussed previously for the smooth tube. In Figure 2 are the results for the local absorbed mass flux as a function of axial location down the tube for the data set ht1-2. The dashed line is for the spiny tube and the solid line is for the smooth tube. Note that the enhancement provided by the spiny tube is not great and

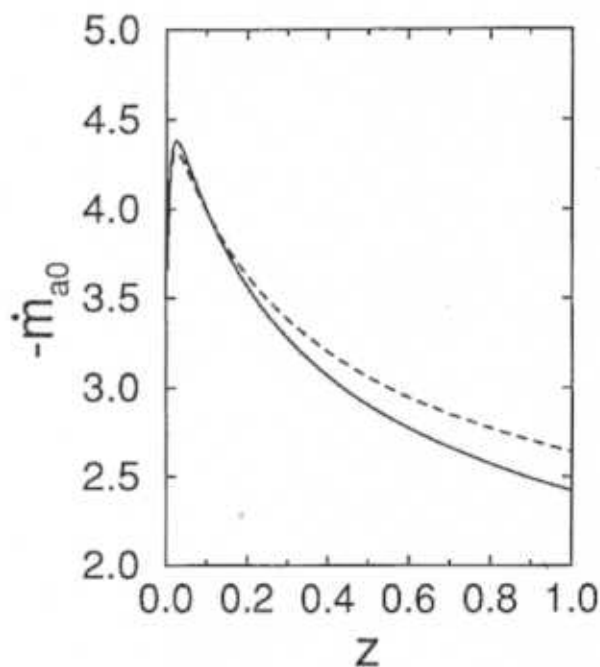


Figure 2 Dimensionless mass flux as a function of distance down the tube for the spiny (dashed curve) and the smooth tube for data set ht1-2.

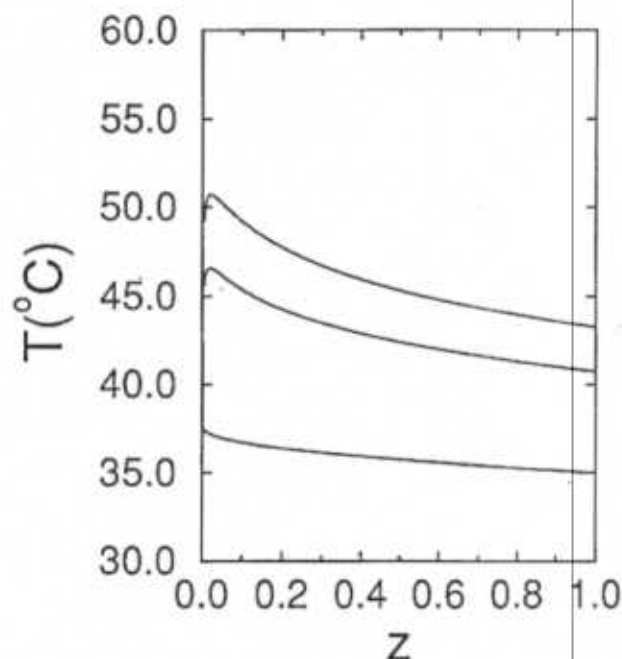


Figure 3 Film (highest), bulk (solution side), and bulk coolant temperature (lowest) as functions of distance down the tube for the data set ht1-2.

TABLE 1 Results for the Spiny Tube Model for the Length of the Spines Being $\frac{1}{32}$ in.*

Data Set	ht1-1	ht1-2	ht2-1	ht2-2	ht3-1	ht3-2
Solution Side						
Mass Fraction LiBr In	.6014	.6252	.6286	.6273	.5927	.6260
Average Mass Fraction LiBr Out						
Experiment	.5796	.6060	.6161	.6118	.5821	.6165
Theory	.5731	.6049	.6130	.6056	.5648	.6130
Theory (smooth)	.5755	.6069	.6150	.6087	.5710	.6158
Film Temperature In (K)	325.44	325.00	329.53	330.45	322.19	325.92
Average Temperature Out						
Experiment	315.45	321.21	324.19	317.47	308.93	323.42
Theory	311.57	313.86	324.91	313.99	312.43	322.36
Theory (smooth)	311.29	313.01	324.14	312.82	311.37	321.34
Mass Absorbed $\frac{kg}{min}$						
Experiment	.0174	.0291	.0082	.0233	.0085	.0139
Theory 1D	.0227	.0309	.0102	.0328	.0229	.0191
Theory 2D	.0188	.0273	.0089	.0292	.0189	.0169
Theory (smooth 1D)	.0207	.0276	.0089	.0281	.0176	.0149
Theory (smooth 2D)	.0172	.0245	.0077	.0250	.0146	.0132
Coolant Side						
Temperature Out						
Experiment	312.24	314.29	325.18	313.55	311.00	321.26
Theory	310.10	310.72	324.24	310.50	310.62	320.42
Theory (smooth)	309.94	310.45	324.13	310.11	310.20	320.08

* No free constants are used in the comparisons

is concentrated in the portion of the tube away from the entrance. The rapid variation of the absorbed mass flux near the entrance is due to the presence of a discontinuity in the mass fraction at the inlet $z = 0$; this discontinuity is discussed in both Conlisk (1992) and Grossman (1983); Conlisk (1992) has shown that the local film thickness near $z = 0$ behaves like $h \sim 1 + A_0 z^d$, where A_0 is a positive constant and d is a positive constant between 0 and 1. From Equation 1 of part I (Conlisk 1996), this behavior leads to an integrable singularity in the mass absorbed.

In Figure 3 are the film surface (highest), solution bulk temperature and coolant bulk temperature (lowest) for the conditions of Figure 2. Here it is noted that the difference between the film and the bulk solution temperature is decreasing slightly with distance down the tube. Note that the bulk coolant temperature varies only mildly; this figure is similar in character to Figure 4 of Patnaik et al. (1993), who present the same temperatures in dimensionless form. It should be noted, however, that due to the one-dimensional nature of that work, the inlet bulk solution temperature is assumed to equal the inlet film surface temperature. Results for the surface and bulk mass fractions (not shown) exhibit similar trends.

Table 1 shows the results for the six data sets whose dimensionless parameters are given in Table 1 of part I. The agreement between theory and experiment for the 1/4-in. pitch tube is relatively good and this seems to coincide with the relatively small value of the local spine parameter $\epsilon_{sp}^3 Ca$ (Table 1 of part I). The outlet solution and coolant temperatures are consistently under-predicted; the reason for this is unknown. As the pitch of the tube becomes smaller, $\epsilon_{sp}^3 Ca$ increases until, for both the data sets having a 1/8-in. pitch, the agreement is poor. This coincides with increasing values of $\epsilon_{sp}^3 Ca$. Table 2 gives the results for the parameter set ht1-2 as a function of the chord of the spines. Note that according to the present model, a longer spine root chord may be advantageous, although a longer chord increases the likelihood that the absorbed mass flux may be reduced due to capillary effects; clearly, there is a trade-off here and this point needs more work. In Table 3 are results for ht1-2 as a function of the number of spine rows for the 1/32-in. spine root chord. Note the monotonic increase in the mass absorbed; also note that a small number of spine rows does not increase the mass absorbed. It should also be noted that the present results agree well with the experimental data presented by Miller and Perez-Blanco (1994) in Table 1 of that work. In particular, the 6.4-mm tube is the 1/4-in. pitch tube quoted here, although some of the other specifications are slightly different. Several runs were made using those data and the result for the total mass absorbed using the full two-dimensional analysis is 0.0118 kg/min, which compares favorably with the experimental value of 0.0110 kg/min obtained by subtracting the mass flow out from the mass flow in rows 12 and 13 of the table in Miller and Perez-Blanco (1994).

TABLE 2 Results for the Spiny Tube Model for the Length of the Spines $1/16$ in. and for $1/32$ in. for the Data Set ht1-2

Spine Length	1/16	1/32
Solution Side		
Average Mass Fraction LiBr Out	.6023	.6047
Average Temperature Out	314.91	313.86
Mass Absorbed ($\frac{\text{kg}}{\text{min}}$; 1D)	.0349	.0309
Mass Absorbed ($\frac{\text{kg}}{\text{min}}$; 2D)	.0309	.0272
Coolant Side		
Temperature Out	311.06	310.72

TABLE 3 Results for the Spiny Tube Model as a Function of the Number of Spine Rows or Pitch for Data Set ht1-2*

Spine Rows	0	60	120	180	240
Solution Side					
Average Mass Fraction LiBr Out	.6069	.6066	.6061	.6056	.6047
Average Temperature Out	313.01	33.14	313.36	313.59	313.86
Mass Absorbed ($\frac{\text{kg}}{\text{min}}$)					
Theory (1D)	.0276	.0282	.0290	.0299	.0309
Theory (2D)	.0245	.0250	.0257	.0265	.0273
Coolant Side					
Temperature Out	310.45	310.50	310.57	310.64	310.72

* The first column is the smooth tube case. The 240-row column is the 1/4 in. pitch case. The spine chord is 1/32 in.

In summary, it is clear that the spiny tube increases the absorbed mass flux when compared with a smooth tube. However, as the experimental data make clear, the enhancement is obtained for only a limited range of pitch and the enhancement is not large. Further analysis suggests that the physical mechanism for the decrease in the mass absorbed for smaller pitch is the capillarity effect caused by surface tension, and this is investigated next.

THE INFLUENCE OF SURFACE TENSION

In the absence of surface tension, the calculated results show a monotonic increase in the mass absorbed as the number of spine rows increases, which is equivalent to the pitch decreasing. On the other hand, the experimental results show a decrease in the mass absorbed as the pitch decreases.

To better understand this phenomenon, additional study of the influence of surface tension has been undertaken. The influence of surface tension can emerge in two distinct ways. First, if the liquid-vapor interface is curved, there is an effect based on the nonzero value of the surface tension coefficient; this effect is termed *capillarity* and is proportional to the capillary number as described in part I. In the present formulation, this effect is

characterized by the capillary number Ca and the local value of ϵ_{sp} , which is the ratio of the film thickness to the pitch of the tube. Second, if the surface tension varies with temperature and mass fraction, there will be an additional circulation set up due to the generation of an additional induced stress. In a pure fluid, the circulation set up by the surface tension gradient with temperature is called the *Marangoni effect*. It should be noted that in the general case, the surface tension coefficient will be a function of the mass fraction and temperature. However, for the present problem, the surface tension gradient will be a function only of temperature gradient because of the linear relationship between mass fraction and temperature in the equilibrium condition at the interface. Also note that the present situation does not, strictly speaking, correspond to classic Marangoni convection since we are dealing with a fluid mixture. In what follows, this fact is denoted by putting the term *Marangoni* in quotes.

For LiBr-H₂O, the surface tension decreases with increasing temperature and decreases with increasing water mass fraction (Luddy 1987; Yao et al. 1991; Hozawa et al. 1991) and for simplicity it is assumed that

$$\sigma = \sigma_0 - \gamma_T(T - T_{Sin}) - \gamma_M(\omega_A - \omega_{A,Sin}), \quad (25)$$

where σ_0 is the surface tension coefficient at $T = T_{Sin}$ and at $\omega_A = \omega_{A,Sin}$; here both γ_T and γ_M are assumed constant. It is recalled that ω_A is the mass fraction of water. The variation of surface tension induces an additional stress at the liquid-vapor interface, leading to a boundary condition at the interface of the form

$$\frac{\partial w}{\partial y} = -\frac{\epsilon Ma \partial \theta}{Pr \partial z} - \frac{\epsilon Ma_m \partial \Omega}{Pr \partial z}. \quad (26)$$

Here Ma and Ma_m are "Marangoni" numbers:

$$Ma = \frac{\gamma_T \Delta T c_p}{k U_0}, \quad Ma_m = \frac{\gamma_M \Delta \omega c_p}{k U_0}. \quad (27)$$

In the global smooth tube variables, $\epsilon Ma \sim .001$ and so the effect of the variation of surface tension with temperature appears negligible; a similar comment applies to the variation of surface tension with mass fraction. In the region between the spines, $\epsilon_{sp} Ma / Pr \sim .05$, which suggests that the influence of the surface tension gradient with temperature is also not important there. A similar result holds for the variation of surface tension with mass fraction using data from Yao et al. (1991). This is consistent with the assertion of Sternling and Scriven (1959), who suggest that a large surface area is required for the "Marangoni" effect to be significant. From this discussion, it does not appear that "Marangoni" convection is significant for the parameters of this problem, and the primary influence of surface tension is in the capillary effect.

As mentioned above, the decrease in the mass absorbed seems to coincide with the growth of the parameter $\epsilon_{sp}^3 Ca$. From Equation 20 of part I (Conlisk 1996), the z -velocity is multiplied by the factor $(1 - \lambda \epsilon_{sp}^3 Ca)$ and so it is reasonable to look for a correction to the total absorbed flux on the local spine scale in the form of

TABLE 4 Results for the Spiny Tube Model as a Function of the Number of Spine Rows or Pitch for Data Set ht3-2*

Spine Rows	0	320	360	400	480
Solution Side					
Average Mass Fraction LiBr Out	.6158	.6155	.6155	.6155	.6158
Average Temperature Out	321.34	321.41	321.43	321.43	321.41
Mass Absorbed $\frac{kg}{min}$					
Theory (1D)	.0149	.0154	.0154	.0153	.0149
Theory (2D)	.0132	.0137	.0137	.0136	.0133
Coolant Side					
Temperature Out	320.08	320.12	320.12	320.12	321.00

* Corrected for the influence of surface tension (capillary). The first column is the smooth tube case. The 480-row column is the $1/8$ in. pitch case. The spine chord is $1/32$ in. and $\lambda=3.0$.

TABLE 5 Results for the Spiny Tube Model as a Function of the Number of Spine Rows or Pitch for Data Set ht1-2*

Spine Length	0	320	360	400	480
Solution Side					
Average Mass Fraction LiBr Out	.6069	.6048	.6047	.6046	.6048
Average Temperature Out	313.01	314.07	314.09	314.17	314.30
Mass Absorbed $\frac{kg}{min}$					
Theory (1D)	.0276	.0311	.0313	.0314	.0310
Theory (2D)	.0245	.0276	.0278	.0279	.0277
Coolant Side					
Temperature Out	310.45	310.74	310.76	310.78	310.76

* Corrected for the influence of surface tension (capillary). The first column is the smooth tube case. The spine chord is $1/32$ in. and $\lambda=3.0$.

$$\dot{m}_{aT, corr} = (1 - \lambda \epsilon_{sp}^3 Ca) \dot{m}_{aT}. \quad (28)$$

Results for the corrected mass absorbed for data set ht3-2 are depicted in Table 4. Note that the maximum value of the mass absorbed is obtained somewhere around a pitch of 3/16 in. (320 spine rows or stages). Similar results are depicted in Table 5 for the data set ht1-2; since the only significant difference between the two data sets is the coolant temperature, we would expect the maximum result to be around the same pitch as that for data set ht3-2 and this is the case. Note that for data set ht3-2, the corrected values agree well with the experimental results. The value of λ , which, strictly speaking, is defined as $\lambda = L_z / L_{sp}$, is somewhat a matter of choice; in the present context, this must be considered as a constant encompassing the overall effects of the pressure gradient and film effects due

to surface tension. Consequently, the value of $\lambda = 3.0$, while realistic for the tube considered, must be viewed as a heuristic estimate of all the effects of surface tension.

The precise reason for the decrease in the mass absorbed as a result of surface tension is a matter for some speculation. It is known that a thinner film is better for mass absorption than a thicker film. To see this, consider the spiny tube component of the mass flux, which is given by Equation 22. In the regime between the spines, the value of D_{1sp} is small. Using the definitions of the dimensionless parameters and the fact that $U_0 = gh_0^2/\nu$, we consider the limiting case of D_{1sp} small; then it is easily shown from Equation 22, along with the asymptotic expansion of the error function (Abramowitz and Stegun 1965) for large argument, that in the region between a pair of spines (i.e., in a spine channel)

$$\dot{m}_a = \epsilon \delta^{1/2} B \dot{m}_{a0} - \frac{\beta_0 (1/2)^{1/2}}{1 - \omega_{ASin}} \left(\frac{\nu D_{AB}}{g L_{sp}} \right)^{1/2} \frac{1}{h_0 \sqrt{z}} \quad (29)$$

where $\beta_0 = \Delta \omega \beta$ and it is readily seen that

$$\dot{m}_a \sim \frac{1}{h_0} + O(1) \text{ for } |D_{1sp}| \text{ small.} \quad (30)$$

At a fixed flow rate as the pitch decreases, because of the increased number of spine rows, the fluid is expected to wick up a given spine. Consequently, the average film thickness may become so thick that the mass absorbed is significantly reduced. Additional work is required to quantify this effect, however.

SUMMARY

In the present work a model for the calculation of the mass absorbed on a spiny tube has been developed. The model is subject to the specification of only a single average heat transfer coefficient on the coolant side. The model requires a minimum of numerical computation, with the mass absorbed given by a single integral that can easily be evaluated numerically by a standard procedure. It has been shown that the total mass absorbed is enhanced for the spiny tube over the smooth-tube result; however, the enhancement is not large and is significantly decreased with increasing influence of surface tension through capillarity.

The geometry of the spiny tube is complicated; moreover, the solution to the absorption problem requires the simultaneous solution of the velocity field and the temperature and mass fraction over the entire tube. As noted in part 1 (Conlisk 1996), the problem near the spines is generally fully three-dimensional. Thus, substantially computational approaches to this problem are not likely to be productive. Thus a rational approach to the solution of the full problem has been sought by evaluation of the various physical effects through calculation of the relevant dimensionless parameters of the flow and heat and mass transfer problems.

In the region between a pair of spines, the mass transfer has been assumed to be governed by a short-length scale correspond-

ing to the pitch of the tube. The magnitude of the dimensionless parameters for heat transfer indicates that a good approximation may be obtained by a simple conduction-dominated problem. Finally, the mass transfer problem may be reduced to a problem similar to the smooth-tube case, where mass transfer takes place only near the liquid-vapor interface.

The influence of surface tension may be felt in two ways: capillarity and the Marangoni effect. It is shown that the dimensionless parameters of the present problem, the Marangoni effect is negligible. On the other hand, the decrease in the mass absorbed for the smaller values of the pitch seems to correlate with the increase of a parameter based on local spine scales $1 - \lambda \epsilon_s$, and the experimental data for the smaller values of the pitch agree well with a simple linear correction factor for a given value of λ . It must be emphasized, however, that the evidence supporting this view is circumstantial only, and a full theoretical prediction for the drop in the mass absorbed cannot yet be given. Qualitative physical reasoning for the drop in absorbed mass may be due to the fact that as more spine rows are added (that is, the pitch of the tube becomes smaller), the average film thickness increases, leading to a smaller value of the absorbed mass flux.

In the present model for the spiny tube the presence of surface waves and their effect on the absorption process have not been considered. This situation is discussed by Conlisk (1992) for the case of a smooth tube, where it is concluded that the low values of the Reynolds number renders the influence of waves negligible (Javdani 1974). Moreover, as noted by Miller and Peiffer (Blanco 1994), no prominent wavy flow was visible in their visualizations. It is expected that the influence of waves on mass transfer will become much more important as the Reynolds number increases.

ACKNOWLEDGMENTS

This work has been supported by Martin-Marietta Energy Services Corporation. Frequent discussions with W.A. Miller have been extremely helpful during the course of this work. Mr. H. Vandenbosch has provided information concerning the geometry of the spiny tubes.

NOMENCLATURE

- A = constant defined just after Equation 10
- A' = constant defined just after Equation 12
- A_{pa} = see discussion following Equation 18
- A_{sp} = constant defined just after Equation 23
- A_r = heat transfer surface area on solution side
- B = $(\omega_{ASin} - \omega_{ABULK}) / (1 - \omega_{ASin})$
- C = constant defined just after Equation 12
- C_1 = constant defining the equilibrium condition at the interface: $\omega_A = C_1 T + C_2$
- C_2 = constant defining the equilibrium condition at the interface: $\omega_A = C_1 T + C_2$
- c_p = specific heat

c_{pcool} = specific heat of the coolant
 D_1 = constant defined just after Equation 16
 D_{AB} = mass diffusion coefficient
 D_{isp} = constant defined just after Equation 23
 E' = constant defined by Equation 4
 Fr = Froude number
 g = acceleration due to gravity
 h = h^*/h_0^*
 h^* = dimensional film thickness
 h_0^* = dimensional film thickness at the inlet
 h_1 = $h = 1 + \delta^{1/2} B h_1 + \dots$
 h_{abs} = heat of absorption
 h_c = convection coefficient in the coolant
 H = constant defined by Equation 15
 Ja = Jakob number = $c_p \Delta T / h_{abs}$
 k = solution thermal conductivity
 k_w = thermal conductivity of the tube wall
 L = tube length
 L_{sp} = spine root chord
 Le = Lewis number = Pr/Sc
 L_z = pitch of the tube
 \dot{m} = dimensionless mass flux
 \dot{m}_a = $\dot{m}_a / \rho U_0$, dimensionless mass absorbed
 \dot{m}_{a0} = defined by $\dot{m}_a = \delta^{1/2} B \dot{m}_{a0} + \dots$
 \dot{m}_{cool} = mass flow rate of coolant
 \dot{m}_{asp} = dimensionless spine tube component of the absorbed mass flux
 \dot{m}_{asp0} = dimensionless scaled spine tube component of the absorbed mass flux
 \dot{m}_{as}^* = dimensional mass absorbed-smooth component (Equation 18)
 \dot{m}_{asp}^* = dimensional mass absorbed spine tube component (Equation 18)
 Ma = thermal Marangoni number; Equation 27
 Ma_m = mass Marangoni number; Equation 27
 \dot{M}_{aT} = total dimensionless mass flux
 M_e = mass absorption enhancement parameter
 nt = number of spine rows
 N_{st} = $nt - 1$
 P_B = defined by Equation 24
 Pr = Prandtl number = $\mu c_p / k$
 q_S = dimensional heat flux at the interface
 Re = Reynolds number = $(U_0 h_0^*) / \nu$
 r_i = inner radius of tube; Figure 1
 r_o = outer radius of tube (solution side); Figure 1
 r_s = inner radius of annulus; Figure 1
 Sc = Schmidt number = ν / D_{AB}
 t = thickness of the tube wall between coolant and film

T_{BC} = bulk coolant temperature
 T_{BCout} = bulk coolant temperature out
 T_{Sin} = film surface temperature at the inlet
 T_W = wall temperature on the film side
 T_{WC} = wall temperature on the coolant side
 T_{Win} = wall temperature at the inlet on the film side
 ΔT = $T_{Sin} - T_{Win}$
 U_0 = gh_0^{*2}/ν , velocity scale
 y = dimensionless coordinate normal to wall; nondimensionalized on h_0^*
 z = dimensionless coordinate in the axial direction; nondimensionalized on the length of the tube

Greek Symbols

α = ρ_w / ρ in the film bulk (constant)
 β = defined by Equation 21
 δ = $1/\epsilon Re Sc$
 δ_{sp} = $1/\epsilon_{sp} Re Sc$
 ϵ = h_0^*/L
 ϵ_{sp} = h_0^*/L_z
 γ = constant defined by Equation 9
 γ_M = see Equation 25
 γ_T = see Equation 25
 ν = mixture kinematic viscosity
 ρ = mixture density
 ρ_w = density of water
 σ = surface tension defined by Equation 25
 σ_0 = $\sigma(T_{Sin}, \omega_{ASin})$ surface tension
 θ = $(T - T_{Win})/\Delta T$
 θ_{BC} = scaled coolant bulk temperature
 θ_S = dimensionless film surface temperature
 θ_W = dimensionless wall temperature
 $\Delta\omega$ = $\omega_{ASin} - \omega_{ABULK}$
 ω_A = mass fraction of species A
 ω_{ABULK} = mass fraction in the bulk; constant
 ω_{ASin} = film surface mass fraction at the inlet
 Ω = $(\omega_A - \omega_{ABULK})/\Delta\omega$

REFERENCES

- Abramowitz, M., and I. Stegun. 1965. *Handbook of mathematical functions*. New York: Dover.
 Conlisk, A.T. 1992. Falling film absorption on a cylindrical tube. *AIChE J.* 38(11): 1716.
 Conlisk, A.T. 1994a. The use of boundary layer techniques in the design of a falling film absorber. International Absorption Heat Pump Conference '94, January 19-21, New Orleans.
 Conlisk, A.T. 1994b. Semi-analytical design of a falling film absorber. *ASME J. Heat Transfer* 116(4): 1055-1058.

- Conlisk, A.T. 1994c. The structure of falling film heat and mass transfer on a fluted tube. *AIChE J.* 40(5): 756-766.
- Conlisk, A.T. 1994d. Analytical solutions for the heat and mass transfer in a falling film absorber. *Chem. Eng. Sci.* 50(4): 651-660.
- Conlisk, A.T. 1995. The effect of coolant flow parameters on the performance of an absorber. *ASHRAE Transactions* 101(2): 73.
- Conlisk, A.T. 1996. Prediction of the performance of a spined-tube absorber—Part I: Governing equations and dimensional analysis. *ASHRAE Transactions* 102(1).
- Grossman, G. 1983. Simultaneous heat and mass transfer in film absorption under laminar flow. *Int. J. Heat Mass Transfer* 26(3): 357-371.
- Hozawa, M., M. Inoue, J. Sato, T. Tsukada, and N. Imaishi. 1991. Marangoni convection during steam absorption into aqueous LiBr solution with surfactant. *J. Chem. Eng. Jap.* 24(2): 209-214.
- Incropera, F.P., and D.P. Dewitt. 1990. *Introduction to heat transfer*, 2d ed. New York: John Wiley and Sons.
- Javdani, K. 1974. Mass transfer in wavy liquid films. *Chem. Eng. Sci.* 29: 61-69.
- Luddy, C. 1987. Surface tension values for two absorption refrigeration pairs: Ammonia-water and water-lithium bromide. M.S. thesis. Columbus: Ohio State University.
- Miller, W.A. 1992. Private communications.
- Miller, W.A. 1993. Private communications.
- Miller, W.A., and H. Pérez-Blanco. 1994. Vertical-tube aqueous LiBr falling film absorption using enhanced surfaces. *International Absorption Heat Pump Conference '94*, January 19-21, New Orleans, pp. 185-202.
- Patnaik, V., H. Pérez-Blanco, and W.A. Ryan. 1993. A simple analytical model for the design of vertical tube absorbers. *ASHRAE Transactions* 99(2): 69-80.
- Sternling, C.V., and L.E. Scriven. 1959. Interfacial turbulence hydrodynamic instability and the Marangoni effect. *AIChE J.* 5(12): 514-523.
- Yao, W., H. Bjurstrom, and F. Setterwall. 1991. Surface tension of lithium bromide solutions with heat-transfer additives. *J. Chem. Eng. Data* 36: 96-98.